JOURNAL OF APPLIED CRYSTALLOGRAPHY

ISSN 1600-5767

Form factor of any polyhedron and its singularities derived from a projection method

Tianjuan Yang, Xiuguo Chen,* Jiahao Zhang, Jianyuan Ma and Shiyuan Liu*

State Key Laboratory of Digital Manufacturing Equipment and Technology, Huazhong University of Science and Technology, 1037 Luoyu Road, Wuhan, Hubei 430074, People's Republic of China. *Correspondence e-mail: xiuguochen@hust.edu.cn, shyliu@hust.edu.cn

Received 16 March 2022
Accepted 23 November 2022

Edited by V. T. Forsyth, Lund University, Sweden, and Keele University, United Kingdom

Keywords: form factors; polyhedra; singularities; small-angle scattering.

An analytical and general form factor for any polyhedron is derived on the basis of a projection method, in terms of the vertex coordinates and topology of the polyhedron. An integral over the polyhedron equals the sum of the signed integrals over a set of dissected tetrahedra by defining a sign function, and a general tetrahedral form factor is established by defining a projection method. All possible singularities present in the formula are discussed in detail. Using a MATLAB implementation, illustrative examples are discussed to verify the accuracy and generality of the method. The use of the scalar product operation and the sign function in this work allows a general and neat formula to be obtained for any polyhedron, including convex and concave polyhedra. The formulas and discussions presented here will be useful for the characterization of nanoparticles using small-angle scattering techniques.

1. Introduction

The nanostructure form factor, $F(\mathbf{q})$, which is the Fourier transform (FT) of the particle shape, is of major importance in the context of small-angle scattering (SAS) techniques, such as small-angle neutron scattering and small-angle X-ray scattering (Senesi & Lee, 2015*a*,*b*; Croset, 2017; Barke *et al.*, 2015). The ability to compute the form factor for a nanoparticle with a complex shape is an important goal in SAS because detailed structural information can only be obtained from SAS when the correct form factor is adopted. Many particle shape transformations have been derived, but only for a limited number of simple particle shapes (Hendricks et al., 1974; Li et al., 2011; Mittelbach & Porod, 1961; Renaud et al., 2009). A complex particle shape in SAS techniques is often approximated as a sphere model, which provides statistically meaningful information but ignores the structural details of the size and shape, limiting the application of SAS techniques (Murray et al., 2000; Lee et al., 2009). In many cases, the use of polyhedral particles may be advantageous over spherical particles, since a detailed description of the shape and size of the nanoparticle can reveal more physical properties that are relevant in many fields: magnetism (Gruner et al., 2008), optics and plasmonics (Langille et al., 2012), and catalysis (Yamada et al., 2011). Therefore, developing an exact and generic form factor for an arbitrary polyhedral nanoparticle is of wide interest and practical significance in SAS techniques.

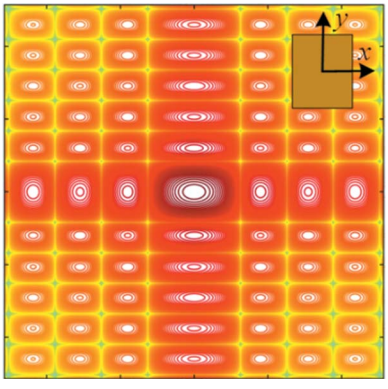

Large collections of nanoparticle transforms have been derived and implemented in SAS software (Li *et al.*, 2011; Engel & Laasch, 2020; Lazzari, 2006; Pospelov *et al.*, 2020; Chourou *et al.*, 2013). Two main solutions have been employed to analytically calculate the form factors of polyhedra: (i) a

direct integration solution, using Fubini's theorem, is suitable for very simple objects with edges along the coordinate axes, such as simple prisms (cube, parallelepiped *etc*.) or simple pyramids (di-rectangular tetrahedron, square pyramid *etc*.); (ii) a generic decomposition solution, which partitions an object into smaller simple objects that are easy to integrate, in terms of topology and vertex coordinates, is suitable for some complex objects (Lien & Kajiya, 1984; Lee & Requicha, 1982). A generic formula for the polyhedral form factor was derived decades ago, but singularities were not discussed (Patterson, 1939). Striking contributions are the form factors of polyhedra established by Croset (2017, 2018), Wuttke (2017, 2021) and Senesi & Lee (2015*a*). Croset established a general and exact formula by performing the calculation on the simplices with vectorial operations, and generalized the result for quite a large class of polyhedra and more rounded bodies by using a cutting procedure; the appeal of this method is that it allows a generic analysis of the singularities. Wuttke presented a different derivation that is based on the use of the divergence theorem and Stokes's theorem to reduce the volume integral to surface integrals, and further reduce surface integrals to straight-line integrals; singularities are cancelled by using series expansions. Senesi & Lee proposed a general decomposition method to calculate the form factors of polyhedra by decomposing a polyhedron into di-rectangular tetrahedral subunits and deriving the polyhedral form factor as the sum of each subunit form factor evaluated at different rotated $\mathbf{q}$, which leads to the limit of the subunit form. Generating an appropriate decomposition for a complex shape and solving the basic problem of evaluating the integral over the subunits are usually the cruces of the decomposition solution, which decide the goals of exactness and ease of implementation.

In this work, we propose a different derivation of the form factor for an arbitrary polyhedron using scalar product operations on vectors and the sign function, and we discuss the singularities from our formula. We first present a general formula to calculate the form factor for an arbitrary tetrahedron via a projection method. Then, any singularity that appears in the formula is discussed in detail and removed. Further, a strategy of the integral over a polyhedron is established systematically by adding a set of signed integrals over the dissected tetrahedra. Finally, illustrative examples are discussed to verify the accuracy and generality of the method. The method described herein is regarded as a supplement to existing methods and will facilitate the characterization of nanomaterials when using SAS techniques.

2. The tetrahedral form factor: principle of the projection method

Definition 1. The form factor of an object, denoted as $F(\mathbf{q})$, which is the FT of the particle defined by volume V, can be described as (Guinier & Fournet, 1955; Roe, 2000; Warren, 1990; Guinier, 1963)

$$F(\mathbf{q}) = \int_V \exp(\mathrm{i}\mathbf{q}\cdot\mathbf{r})\,\mathrm{d}r, \tag{1}$$

where $\mathbf{q}$ is the scattering vector and $\mathbf{r}$ is a position vector.

Definition 2. The scattering intensity is proportional to the form factor amplitude for the individual particle:

$$I(\mathbf{q}) \propto \left|F(\mathbf{q})\right|^2. \tag{2}$$

The formula mentioned above will be used to calculate SAS images from individual three-dimensional particles discussed in this work, as it allows the extraction of relevant structural information from a single scattering pattern of an individual particle, provided that the particle can be adequately described by a parameterized geometric model. The computation of SAS from an assembled system composed of multiple types of particles (such as a single-component monodisperse system, a single-component polydisperse system, a multi-component monodisperse system, a multi-component polydisperse system, crystal structure *etc*.) is an interesting and important question, although beyond the scope of the present work.

The basic subunit of a polyhedron is the tetrahedron, and the integration over the polyhedron equals the sum of the integrations over all tetrahedra, according to the linearity property of the FT. However, one must first solve the basic problem of evaluating an integral over the tetrahedron. For an orthogonal unit tetrahedron, it is straightforward to derive the form factor by Fubini's theorem. As a consequence, a projection method that has been widely used for deriving the volume, mass or moment of inertia of a solid is adopted in this work for deriving the form factor of an arbitrary tetrahedron.

The form factor in equation (1) can be described by the coordinate components:

$$\begin{aligned} F(\mathbf{q}) &= \int_V \exp(\mathrm{i}\mathbf{q}\cdot\mathbf{r})\,\mathrm{d}r \\ &= \int_V \exp\left[\mathrm{i}(q_x x + q_y y + q_z z)\right]\mathrm{d}x\,\mathrm{d}y\,\mathrm{d}z. \end{aligned} \tag{3}$$

Proposition 1. The form factor for an arbitrary tetrahedron given by its four vertices ($\mathbf{v}_0$, $\mathbf{v}_1$, $\mathbf{v}_2$, $\mathbf{v}_3$), where $\mathbf{v}_0$ is located at the projection origin and $\mathbf{v}_1$, $\mathbf{v}_2$, $\mathbf{v}_3$ are specified in the sequence so that the normal vector of the face always points away from the tetrahedron, can be conveniently computed from

$$\begin{aligned} F_{\mathrm{tetra}}(\mathbf{q}) = \left|\det(\mathbf{T})\right| \Bigg\{ & \frac{\mathrm{i}}{(\mathbf{q}\cdot\mathbf{v}_1)(\mathbf{q}\cdot\mathbf{v}_1 - \mathbf{q}\cdot\mathbf{v}_2)(\mathbf{q}\cdot\mathbf{v}_1 - \mathbf{q}\cdot\mathbf{v}_3)} \\ & \times \exp[\mathrm{i}(\mathbf{q}\cdot\mathbf{v}_1)] + \frac{\mathrm{i}}{(\mathbf{q}\cdot\mathbf{v}_2)(\mathbf{q}\cdot\mathbf{v}_2 - \mathbf{q}\cdot\mathbf{v}_1)(\mathbf{q}\cdot\mathbf{v}_2 - \mathbf{q}\cdot\mathbf{v}_3)} \\ & \times \exp\left[\mathrm{i}(\mathbf{q}\cdot\mathbf{v}_2)\right] + \frac{\mathrm{i}}{(\mathbf{q}\cdot\mathbf{v}_3)(\mathbf{q}\cdot\mathbf{v}_3 - \mathbf{q}\cdot\mathbf{v}_2)(\mathbf{q}\cdot\mathbf{v}_3 - \mathbf{q}\cdot\mathbf{v}_1)} \\ & \times \exp\left[\mathrm{i}(\mathbf{q}\cdot\mathbf{v}_3)\right] + \frac{-\mathrm{i}}{(\mathbf{q}\cdot\mathbf{v}_1)(\mathbf{q}\cdot\mathbf{v}_2)(\mathbf{q}\cdot\mathbf{v}_3)} \Bigg\}, \end{aligned} \tag{4}$$

in which

$$\mathbf{q}\cdot\mathbf{v}_i = q_x x_i + q_y y_i + q_z z_i, \quad i = 1, 2, 3, \tag{5}$$

and $|\det(\mathbf{T})|$ is the absolute value of the determinant of the matrix $\mathbf{T}$:

$$\mathbf{T} = \begin{bmatrix} x_1 & x_2 & x_3 \\ y_1 & y_2 & y_3 \\ z_1 & z_2 & z_3 \end{bmatrix}. \tag{6}$$

Proof. Consider an arbitrary tetrahedron with four vertices: $\mathbf{v}_0$ $(0, 0, 0)$, $\mathbf{v}_1$ (x_1, y_1, z_1), $\mathbf{v}_2$ (x_2, y_2, z_2), $\mathbf{v}_3$ (x_3, y_3, z_3). Taking $\mathbf{v}_0$ as the projection origin, we define a linear transformation matrix $\mathbf{T}$ which relates the old coordinate system (x, y, z) to the new system (x', y', z') by

$$\begin{bmatrix} x \\ y \\ z \end{bmatrix} = \mathbf{T}\begin{bmatrix} x' \\ y' \\ z' \end{bmatrix} = \begin{bmatrix} x_1 & x_2 & x_3 \\ y_1 & y_2 & y_3 \\ z_1 & z_2 & z_3 \end{bmatrix}\begin{bmatrix} x' \\ y' \\ z' \end{bmatrix}. \tag{7}$$

Under this transformation, an arbitrary tetrahedron in the old coordinate system (x, y, z) can be projected to the orthogonal unit tetrahedron in the new coordinate system (x', y', z') with coordinates $\mathbf{v}_0'(0, 0, 0)$, $\mathbf{v}_1'(1, 0, 0)$, $\mathbf{v}_2'(0, 1, 0)$, $\mathbf{v}_3'(0, 0, 1)$. According to this transformation, equation (3) becomes

$$\begin{aligned} F(\mathbf{q}) &= \int_V \exp\left[\mathrm{i}(q_x x + q_y y + q_z z)\right] \mathrm{d}x\,\mathrm{d}y\,\mathrm{d}z \\ &= \int_V \exp\left[\mathrm{i}(\mathbf{q}\cdot\mathbf{v}_1)x' + \mathrm{i}(\mathbf{q}\cdot\mathbf{v}_2)y'\right. \\ &\quad \left. + \mathrm{i}(\mathbf{q}\cdot\mathbf{v}_3)z'\right] \left|\frac{(\mathrm{d}x, \mathrm{d}y, \mathrm{d}z)}{(\mathrm{d}x', \mathrm{d}y', \mathrm{d}z')}\right| \mathrm{d}x'\,\mathrm{d}y'\,\mathrm{d}z' \\ &= \left|\det(\mathbf{T})\right| \int_V \exp\left[\mathrm{i}(\mathbf{q}\cdot\mathbf{v}_1)x' + \mathrm{i}(\mathbf{q}\cdot\mathbf{v}_2)y'\right. \\ &\quad \left. + \mathrm{i}(\mathbf{q}\cdot\mathbf{v}_3)z'\right] \mathrm{d}x'\,\mathrm{d}y'\,\mathrm{d}z' \\ &= \left|\det(\mathbf{T})\right| \int_0^1 \int_0^{1-z'} \int_0^{1-z'-y'} \exp\left[\mathrm{i}(\mathbf{q}\cdot\mathbf{v}_1)x'\right. \\ &\quad \left. + \mathrm{i}(\mathbf{q}\cdot\mathbf{v}_2)y' + \mathrm{i}(\mathbf{q}\cdot\mathbf{v}_3)z'\right] \mathrm{d}x'\,\mathrm{d}y'\,\mathrm{d}z'. \end{aligned} \tag{8}$$

Since the integral region is defined as positively oriented in this work, we take the absolute value of the determinant of the matrix $\mathbf{T}$ in the integration to ensure that the volume integration is always positive in the coordinate transformations.

Finally, we present the integral over an orthogonal unit tetrahedron based on the above transformation:

$$\begin{aligned} F_{\mathrm{tetra}}(\mathbf{q}) &= \left|\det(\mathbf{T})\right| \int_0^1 \int_0^{1-z'} \int_0^{1-z'-y'} \exp\left[\mathrm{i}(\mathbf{q}\cdot\mathbf{v}_1)x'\right. \\ &\quad \left. + \mathrm{i}(\mathbf{q}\cdot\mathbf{v}_2)y' + \mathrm{i}(\mathbf{q}\cdot\mathbf{v}_3)z'\right] \mathrm{d}x'\,\mathrm{d}y'\,\mathrm{d}z' \\ &= \left|\det(\mathbf{T})\right| \int_0^1 \exp\left[\mathrm{i}(\mathbf{q}\cdot\mathbf{v}_3)z'\right] \mathrm{d}z' \int_0^{1-z'} \exp\left[\mathrm{i}(\mathbf{q}\cdot\mathbf{v}_2)y'\right] \mathrm{d}y' \\ &\quad \times \int_0^{1-z'-y'} \exp\left[\mathrm{i}(\mathbf{q}\cdot\mathbf{v}_1)x'\right] \mathrm{d}x' \\ &= \left|\det(\mathbf{T})\right| \left\{ \frac{\mathrm{i}}{(\mathbf{q}\cdot\mathbf{v}_1)(\mathbf{q}\cdot\mathbf{v}_1 - \mathbf{q}\cdot\mathbf{v}_2)(\mathbf{q}\cdot\mathbf{v}_1 - \mathbf{q}\cdot\mathbf{v}_3)} \right. \\ &\quad \times \exp\left[\mathrm{i}(\mathbf{q}\cdot\mathbf{v}_1)\right] + \frac{\mathrm{i}}{(\mathbf{q}\cdot\mathbf{v}_2)(\mathbf{q}\cdot\mathbf{v}_2 - \mathbf{q}\cdot\mathbf{v}_1)(\mathbf{q}\cdot\mathbf{v}_2 - \mathbf{q}\cdot\mathbf{v}_3)} \\ &\quad \times \exp\left[\mathrm{i}(\mathbf{q}\cdot\mathbf{v}_2)\right] + \frac{\mathrm{i}}{(\mathbf{q}\cdot\mathbf{v}_3)(\mathbf{q}\cdot\mathbf{v}_3 - \mathbf{q}\cdot\mathbf{v}_2)(\mathbf{q}\cdot\mathbf{v}_3 - \mathbf{q}\cdot\mathbf{v}_1)} \\ &\quad \left. \times \exp\left[\mathrm{i}(\mathbf{q}\cdot\mathbf{v}_3)\right] + \frac{-\mathrm{i}}{(\mathbf{q}\cdot\mathbf{v}_1)(\mathbf{q}\cdot\mathbf{v}_2)(\mathbf{q}\cdot\mathbf{v}_3)} \right\}. \end{aligned} \tag{9}$$

Remark 1. The volume integral can be represented as a surface integral over the boundary of the tetrahedron, which is consistent with the divergence theorem. Let us call the face to which $\mathbf{v}_1$, $\mathbf{v}_2$ and $\mathbf{v}_3$ belong the base of the tetrahedron, with respect to the origin $\mathbf{v}_0$. With this projection method, there is no need to further decompose a tetrahedron into many di-rectangular tetrahedra, as assumed by Senesi & Lee (2015*a*).

Remark 2. The analytic form factor (4) shows that there are some problems for computer implementation: division by zero at the singularities and loss of arithmetic precision near the singularities. Proper treatment of the formula that takes care of these singularities would be more practical for computing form factors at arbitrary wavevectors.

3. Statements about the singularities

As mentioned above, there exist some directions of $\mathbf{q}$ for which the form factor presents singularities for computer implementation: $\mathbf{q}$ may tend to zero, $\mathbf{q}$ may be perpendicular to a point ($\mathbf{q}\cdot\mathbf{v}_i = 0$, $i = 1, 2, 3$), $\mathbf{q}$ may be perpendicular to a single edge ($\mathbf{q}\cdot\mathbf{v}_i - \mathbf{q}\cdot\mathbf{v}_j = 0$, $i, j = 1, 2, 3$) or $\mathbf{q}$ may be perpendicular to a face ($\mathbf{q}\cdot\mathbf{v}_i - \mathbf{q}\cdot\mathbf{v}_j = \mathbf{q}\cdot\mathbf{v}_i - \mathbf{q}\cdot\mathbf{v}_k = 0$, $i, j, k = 1, 2, 3$). Croset (2017) suggested that the degree of this singularity is closely related to the asymptotic envelope of $F(\mathbf{q})$ for different $\mathbf{q}$ directions, which goes as q^{-3}, q^{-2} or q^{-1} depending on whether $\mathbf{q}$ is large, $\mathbf{q}$ is perpendicular to an edge or $\mathbf{q}$ is perpendicular to a face. Then, Croset (2018) rederived the asymptotic behaviour by using the sections method. Wuttke (2021) used series expansions to overcome numeric

instabilities for small $\mathbf{q}$ and $q_{\|}$. Wuttke pointed out that $F(\mathbf{q})$ is a holomorphic function of each Cartesian component of $\mathbf{q}$; therefore any apparent singularity is removable. In this section, we present some different derivations which can overcome numeric instabilities from our proposed formula.

3.1. q perpendicular to a point's position vector

Proposition 2. If it happens that a given vector $\mathbf{q}$ is exactly or almost perpendicular to a point's position vector $\mathbf{v}_i$ ($\mathbf{q}\cdot\mathbf{v}_i = 0$, $i = 1, 2, 3$) without being normal to either the edge or the face to which this point belongs, the analytic form factor becomes

$$F_{\rm P}(\mathbf{q}) = \left|\det(\mathbf{T})\right|\Big\{\frac{\mathrm{i}}{(\mathbf{q}\cdot\mathbf{v}_j)^2(\mathbf{q}\cdot\mathbf{v}_j-\mathbf{q}\cdot\mathbf{v}_k)} \times \exp\big[\mathrm{i}(\mathbf{q}\cdot\mathbf{v}_j)\big] + \frac{\mathrm{i}}{(\mathbf{q}\cdot\mathbf{v}_k)^2(\mathbf{q}\cdot\mathbf{v}_k-\mathbf{q}\cdot\mathbf{v}_j)} \times \exp\big[\mathrm{i}(\mathbf{q}\cdot\mathbf{v}_k)\big] + \frac{\mathrm{i}(\mathbf{q}\cdot\mathbf{v}_j+\mathbf{q}\cdot\mathbf{v}_k)-(\mathbf{q}\cdot\mathbf{v}_j)(\mathbf{q}\cdot\mathbf{v}_k)}{(\mathbf{q}\cdot\mathbf{v}_j)^2(\mathbf{q}\cdot\mathbf{v}_k)^2}\Big\}, \tag{10}$$

where $\mathbf{v}_j$, $\mathbf{v}_k$ are the two other points besides $\mathbf{v}_i$ ($i = 1, 2, 3$).

Proof. For this purpose, we consider the following case when $\mathbf{q}\cdot\mathbf{v}_1 = 0$. Recalling the integral expression (8) of the form factor, we have

$$\begin{aligned} F_{\rm P}(\mathbf{q}) &= \left|\det(\mathbf{T})\right| \int_0^1 \int_0^{1-z'} \int_0^{1-z'-y'} \exp\big[\mathrm{i}(\mathbf{q}\cdot\mathbf{v}_1)x' + \mathrm{i}(\mathbf{q}\cdot\mathbf{v}_2)y' + \mathrm{i}(\mathbf{q}\cdot\mathbf{v}_3)z'\big]\,\mathrm{d}x'\,\mathrm{d}y'\,\mathrm{d}z' \\ &= \left|\det(\mathbf{T})\right| \int_0^1 \exp\big[\mathrm{i}(\mathbf{q}\cdot\mathbf{v}_3)z'\big]\,\mathrm{d}z' \int_0^{1-z'} \exp\big[\mathrm{i}(\mathbf{q}\cdot\mathbf{v}_2)y'\big]\,\mathrm{d}y' \times \int_0^{1-z'-y'} 1\,\mathrm{d}x' \\ &= \left|\det(\mathbf{T})\right|\Big\{\frac{\mathrm{i}}{(\mathbf{q}\cdot\mathbf{v}_2)^2(\mathbf{q}\cdot\mathbf{v}_2-\mathbf{q}\cdot\mathbf{v}_3)} \times \exp\big[\mathrm{i}(\mathbf{q}\cdot\mathbf{v}_2)\big] + \frac{\mathrm{i}}{(\mathbf{q}\cdot\mathbf{v}_3)^2(\mathbf{q}\cdot\mathbf{v}_3-\mathbf{q}\cdot\mathbf{v}_2)} \times \exp\big[\mathrm{i}(\mathbf{q}\cdot\mathbf{v}_3)\big] + \frac{\mathrm{i}(\mathbf{q}\cdot\mathbf{v}_2+\mathbf{q}\cdot\mathbf{v}_3)-(\mathbf{q}\cdot\mathbf{v}_2)(\mathbf{q}\cdot\mathbf{v}_3)}{(\mathbf{q}\cdot\mathbf{v}_2)^2(\mathbf{q}\cdot\mathbf{v}_3)^2}\Big\}. \end{aligned} \tag{11}$$

Similar results can be obtained by performing the same operations for the other two cases when $\mathbf{q}\cdot\mathbf{v}_2 = 0$ and when $\mathbf{q}\cdot\mathbf{v}_3 = 0$. Finally, we obtained formula (10).

To illustrate the loss of arithmetic accuracy near the singularity ($\mathbf{q}\cdot\mathbf{v}_i = 0$), Fig. 1 compares formula (10) with formula (4) for a tetrahedral form factor. For $|\mathbf{q}\cdot\mathbf{v}_i|$ close to or below 10^{-9}, the results obtained from formula (4) show numeric instabilities while formula (10) works well. There is a wide range above 10^{-9} where the two methods are in good agreement. In practice, if $|\mathbf{q}\cdot\mathbf{v}_i/\mathbf{q}\cdot\mathbf{v}_m|$ ($m = j, k$) is close to the machine epsilon, then it is adequate to let $\mathbf{q}\cdot\mathbf{v}_i = 0$.

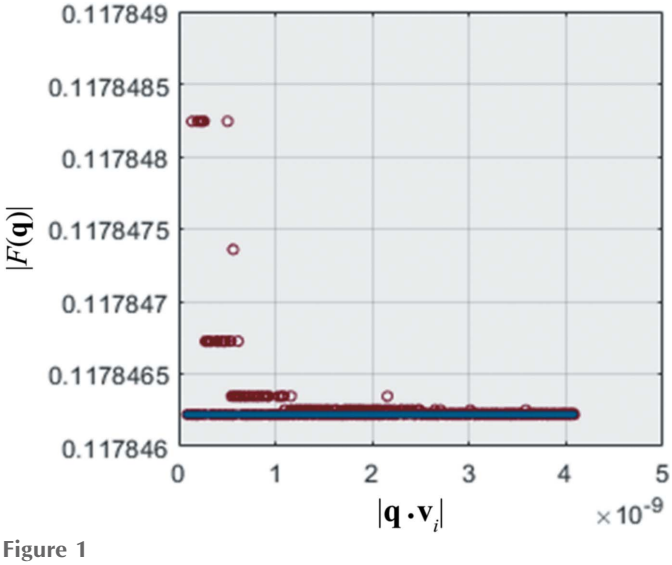

Figure 1
The plot shows the form factor versus $|\mathbf{q}\cdot\mathbf{v}_i|$ for a tetrahedron at the off-symmetric direction $(1, 2, 3)/14^{1/2}$ (the base is an equilateral triangle in the xy plane, oriented so that an edge points in the x direction, with edge length $L = 1$). Red circles are computed using formula (4). For $|\mathbf{q}\cdot\mathbf{v}_i| < 10^{-9}$ ($|\mathbf{q}\cdot\mathbf{v}_i/\mathbf{q}\cdot\mathbf{v}_m| < 10^{-8}$, $m = j, k$), round-off errors dominate. The blue line is computed by formula (10).

3.2. q perpendicular to an edge

Proposition 3. When $\mathbf{q}$ is exactly or almost perpendicular to the edge $\mathbf{v}_i\mathbf{v}_j$ without being normal to the face to which this edge belongs, we have $\mathbf{q}\cdot\mathbf{v}_i - \mathbf{q}\cdot\mathbf{v}_j = 0$, that is $\mathbf{q}\cdot\mathbf{v}_i = \mathbf{q}\cdot\mathbf{v}_j$ ($i = 1, 2, 3$), and the analytic form factor becomes

$$F_{\rm E}(\mathbf{q}) = \left|\det(\mathbf{T})\right|\Big\{\frac{\mathrm{i}}{(\mathbf{q}\cdot\mathbf{v}_k)(\mathbf{q}\cdot\mathbf{v}_k-\mathbf{q}\cdot\mathbf{v}_i)^2} \times \exp\big[\mathrm{i}(\mathbf{q}\cdot\mathbf{v}_k)\big] - \frac{\mathrm{i}}{(\mathbf{q}\cdot\mathbf{v}_i)^2(\mathbf{q}\cdot\mathbf{v}_k)} + \frac{\mathrm{i}(\mathbf{q}\cdot\mathbf{v}_k)-2\mathrm{i}(\mathbf{q}\cdot\mathbf{v}_i)-(\mathbf{q}\cdot\mathbf{v}_i)^2+(\mathbf{q}\cdot\mathbf{v}_i)(\mathbf{q}\cdot\mathbf{v}_k)}{(\mathbf{q}\cdot\mathbf{v}_i)^2(\mathbf{q}\cdot\mathbf{v}_k-\mathbf{q}\cdot\mathbf{v}_i)^2} \times \exp\big[\mathrm{i}(\mathbf{q}\cdot\mathbf{v}_i)\big]\Big\}, \tag{12}$$

where $\mathbf{v}_k$ is the other point besides $\mathbf{v}_i$ and $\mathbf{v}_j$.

Proof. Without loss of generality, let us study the case when $\mathbf{q}\cdot\mathbf{v}_1 = \mathbf{q}\cdot\mathbf{v}_2$. Substituting $\mathbf{q}\cdot\mathbf{v}_1$ for $\mathbf{q}\cdot\mathbf{v}_2$ (or substituting $\mathbf{q}\cdot\mathbf{v}_2$ for $\mathbf{q}\cdot\mathbf{v}_1$), the analytic form factor can be computed as

$$
\begin{aligned}
F_{\rm E}(\mathbf{q}) &= \left|\det(\mathbf{T})\right| \int_0^1 \int_0^{1-z'} \int_0^{1-z'-y'} \exp\left[\mathrm{i}(\mathbf{q}\cdot\mathbf{v}_1)x' + \mathrm{i}(\mathbf{q}\cdot\mathbf{v}_2)y' \right. \\
&\quad \left. + \mathrm{i}(\mathbf{q}\cdot\mathbf{v}_3)z'\right] \mathrm{d}x'\,\mathrm{d}y'\,\mathrm{d}z' \\
&= \left|\det(\mathbf{T})\right| \int_0^1 \exp\left[\mathrm{i}(\mathbf{q}\cdot\mathbf{v}_3)z'\right] \mathrm{d}z' \int_0^{1-z'} \exp\left[\mathrm{i}(\mathbf{q}\cdot\mathbf{v}_1)y'\right] \mathrm{d}y' \\
&\quad \times \int_0^{1-z'-y'} \exp\left[\mathrm{i}(\mathbf{q}\cdot\mathbf{v}_1)x'\right] \mathrm{d}x' \\
&= \left|\det(\mathbf{T})\right| \left\{ \frac{\mathrm{i}}{(\mathbf{q}\cdot\mathbf{v}_3)(\mathbf{q}\cdot\mathbf{v}_3 - \mathbf{q}\cdot\mathbf{v}_1)^2} \right. \\
&\quad \times \exp\left[\mathrm{i}(\mathbf{q}\cdot\mathbf{v}_3)\right] - \frac{\mathrm{i}}{(\mathbf{q}\cdot\mathbf{v}_1)^2(\mathbf{q}\cdot\mathbf{v}_3)} \\
&\quad + \frac{\mathrm{i}(\mathbf{q}\cdot\mathbf{v}_3) - 2\mathrm{i}(\mathbf{q}\cdot\mathbf{v}_1) - (\mathbf{q}\cdot\mathbf{v}_1)^2 + (\mathbf{q}\cdot\mathbf{v}_1)(\mathbf{q}\cdot\mathbf{v}_3)}{(\mathbf{q}\cdot\mathbf{v}_1)^2(\mathbf{q}\cdot\mathbf{v}_3 - \mathbf{q}\cdot\mathbf{v}_1)^2} \\
&\quad \left. \times \exp\left[\mathrm{i}(\mathbf{q}\cdot\mathbf{v}_1)\right] \right\}. \qquad (13)
\end{aligned}
$$

Similar results can be obtained by performing the same operations for the other two cases when $\mathbf{q}\cdot\mathbf{v}_1 = \mathbf{q}\cdot\mathbf{v}_3$ and when $\mathbf{q}\cdot\mathbf{v}_2 = \mathbf{q}\cdot\mathbf{v}_3$. Finally, we obtained formula (12).

To illustrate the loss of arithmetic accuracy near the singularity ($\mathbf{q}\cdot\mathbf{v}_i = \mathbf{q}\cdot\mathbf{v}_j$), Fig. 2 compares formula (12) with formula (4) for the same tetrahedral form factor as in Fig. 1. For $|\mathbf{q}\cdot\mathbf{v}_i - \mathbf{q}\cdot\mathbf{v}_j|$ below 10^{-10}, results obtained from formula (4) show numeric instabilities while formula (12) works well, and there is a wide range above 10^{-10} where the two methods are in good agreement. In practice, if $|\mathbf{q}\cdot\mathbf{v}_i - \mathbf{q}\cdot\mathbf{v}_j|$ is smaller than the machine epsilon, then it is adequate to let $\mathbf{q}\cdot\mathbf{v}_i = \mathbf{q}\cdot\mathbf{v}_j$.

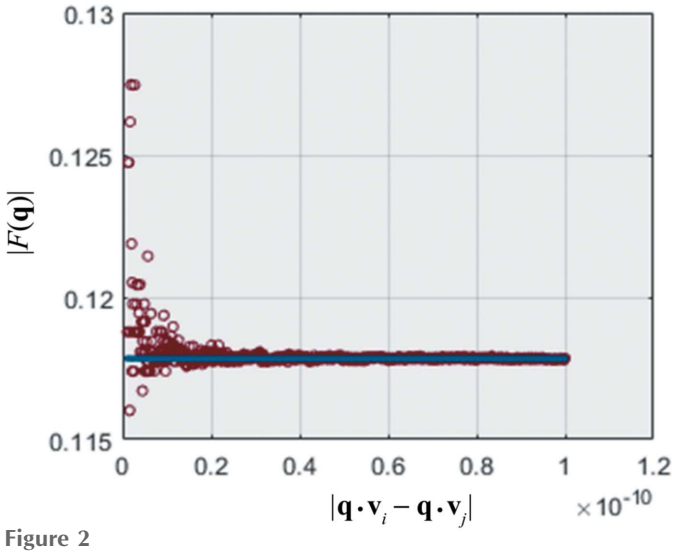

Figure 2
The plot shows the form factor versus the difference between $\mathbf{q}\cdot\mathbf{v}_i$ and $\mathbf{q}\cdot\mathbf{v}_j$ for the same tetrahedron as in Fig. 1. Red circles are computed using formula (4). For $|\mathbf{q}\cdot\mathbf{v}_i - \mathbf{q}\cdot\mathbf{v}_j| < 10^{-10}$, round-off errors dominate. The blue line is computed by formula (12).

3.3. q perpendicular to a face

Proposition 4. When $\mathbf{q}$ is exactly or almost perpendicular to a face specified by its three vertices $\mathbf{v}_i$ ($i = 1, 2, 3$) without being zero, we have $\mathbf{q}\cdot\mathbf{v}_i - \mathbf{q}\cdot\mathbf{v}_j = \mathbf{q}\cdot\mathbf{v}_i - \mathbf{q}\cdot\mathbf{v}_k = 0$, that is $\mathbf{q}\cdot\mathbf{v}_i = \mathbf{q}\cdot\mathbf{v}_j = \mathbf{q}\cdot\mathbf{v}_k$, and the analytic form factor can be expressed by the following formula:

$$
\begin{aligned}
F_{\rm F}(\mathbf{q}) &= \left|\det(\mathbf{T})\right| \left\{ \frac{-\mathrm{i}}{(\mathbf{q}\cdot\mathbf{v}_i)^3} + \frac{2\mathrm{i} + 2(\mathbf{q}\cdot\mathbf{v}_i) - \mathrm{i}(\mathbf{q}\cdot\mathbf{v}_i)^2}{2(\mathbf{q}\cdot\mathbf{v}_i)^3} \right. \\
&\quad \left. \times \exp\left[\mathrm{i}(\mathbf{q}\cdot\mathbf{v}_i)\right] \right\}. \qquad (14)
\end{aligned}
$$

The formula can be expressed by three alternatives (*i.e.* $\mathbf{q}\cdot\mathbf{v}_i = \mathbf{q}\cdot\mathbf{v}_1$ or $\mathbf{q}\cdot\mathbf{v}_i = \mathbf{q}\cdot\mathbf{v}_2$ or $\mathbf{q}\cdot\mathbf{v}_i = \mathbf{q}\cdot\mathbf{v}_3$).

Proof. Substituting $\mathbf{q}\cdot\mathbf{v}_1$for $\mathbf{q}\cdot\mathbf{v}_2$ and $\mathbf{q}\cdot\mathbf{v}_3$, the analytic form factor can be reduced to the following form:

$$
\begin{aligned}
F_{\rm F}(\mathbf{q}) &= \left|\det(\mathbf{T})\right| \int_0^1 \int_0^{1-z'} \int_0^{1-z'-y'} \exp\left[\mathrm{i}(\mathbf{q}\cdot\mathbf{v}_1)x' + \mathrm{i}(\mathbf{q}\cdot\mathbf{v}_2)y' \right. \\
&\quad \left. + \mathrm{i}(\mathbf{q}\cdot\mathbf{v}_3)z'\right] \mathrm{d}x'\,\mathrm{d}y'\,\mathrm{d}z' \\
&= \left|\det(\mathbf{T})\right| \int_0^1 \exp\left[\mathrm{i}(\mathbf{q}\cdot\mathbf{v}_1)z'\right] \mathrm{d}z' \int_0^{1-z'} \exp\left[\mathrm{i}(\mathbf{q}\cdot\mathbf{v}_1)y'\right] \mathrm{d}y' \\
&\quad \times \int_0^{1-z'-y'} \exp\left[\mathrm{i}(\mathbf{q}\cdot\mathbf{v}_1)x'\right] \mathrm{d}x' \\
&= \left|\det(\mathbf{T})\right| \left\{ \frac{-\mathrm{i}}{(\mathbf{q}\cdot\mathbf{v}_1)^3} + \frac{2\mathrm{i} + 2(\mathbf{q}\cdot\mathbf{v}_1) - \mathrm{i}(\mathbf{q}\cdot\mathbf{v}_1)^2}{2(\mathbf{q}\cdot\mathbf{v}_1)^3} \right. \\
&\quad \left. \times \exp\left[\mathrm{i}(\mathbf{q}\cdot\mathbf{v}_1)\right] \right\}. \qquad (15)
\end{aligned}
$$

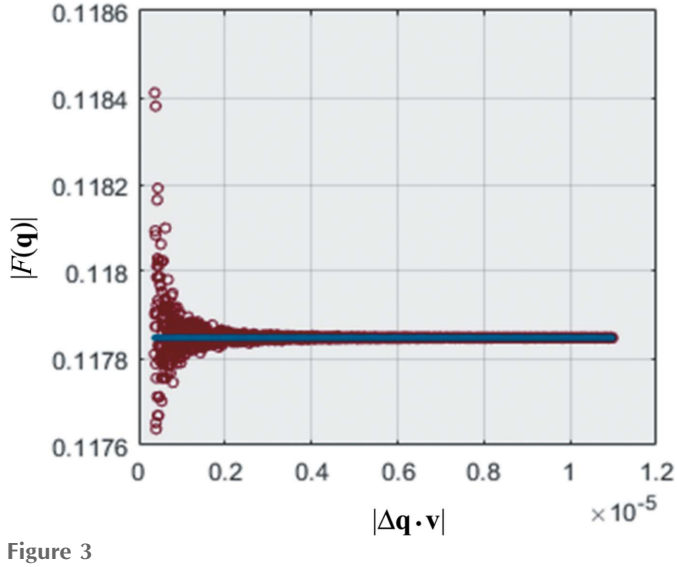

Figure 3
The plot shows the form factor versus the difference $|\Delta\mathbf{q}\cdot\mathbf{v}|$ between $\mathbf{q}\cdot\mathbf{v}_i$, $\mathbf{q}\cdot\mathbf{v}_j$ and $\mathbf{q}\cdot\mathbf{v}_k$ for the same tetrahedron as in Fig. 1. Red circles are computed using formula (4). For $|\Delta\mathbf{q}\cdot\mathbf{v}| < 10^{-5}$, round-off errors dominate. The blue line is computed by formula (14).

The singularity is removed in this case and two other expressions can be used as alternatives for the same case.

To illustrate the loss of arithmetic accuracy near the singularity ($\mathbf{q}\cdot\mathbf{v}_i=\mathbf{q}\cdot\mathbf{v}_j=\mathbf{q}\cdot\mathbf{v}_k$), Fig. 3 compares formula (14) with formula (4) for the same tetrahedral form factor as in Fig. 1. For the difference between $\mathbf{q}\cdot\mathbf{v}_i$, $\mathbf{q}\cdot\mathbf{v}_j$ and $\mathbf{q}\cdot\mathbf{v}_k$ below 10^{-5} ($|\Delta\mathbf{q}\cdot\mathbf{v}|<10^{-5}$), results obtained from formula (4) show numeric instabilities while formula (14) works well, and there is a range above 10^{-5} where the two methods are in good agreement. In practice, if $|\Delta\mathbf{q}\cdot\mathbf{v}|$ is smaller than the machine epsilon, then it is adequate to let $\mathbf{q}\cdot\mathbf{v}_i=\mathbf{q}\cdot\mathbf{v}_j=\mathbf{q}\cdot\mathbf{v}_k$.

3.4. q tends to zero

Proposition 5. When $\mathbf{q}$ tends to zero, an approximate expression of the form factor can be given with the following formula:

$$F_{\rm V}(\mathbf{q})=V_{\rm plhd}+\left|\det(\mathbf{T})\right|\frac{{\rm i}(\mathbf{q}\cdot\mathbf{v}_1+\mathbf{q}\cdot\mathbf{v}_2+\mathbf{q}\cdot\mathbf{v}_3)}{24}, \qquad (16)$$

where $V_{\rm plhd}$ is the volume of the polyhedron.

Proof. When $\mathbf{q}$ is relatively small, rounding errors can grossly distort the form factor. As a remedy, we compute the form factor for small $\mathbf{q}$ by performing a first-order Taylor expansion of formula (4):

$$\begin{aligned}F_{\rm V}(\mathbf{q})&=\left|\det(\mathbf{T})\right|\int_0^1\int_0^{1-z'}\int_0^{1-z'-y'}\exp\left[{\rm i}(\mathbf{q}\cdot\mathbf{v}_1)x'+{\rm i}(\mathbf{q}\cdot\mathbf{v}_2)y'\right.\\&\quad\left.+{\rm i}(\mathbf{q}\cdot\mathbf{v}_3)z'\right]{\rm d}x'\,{\rm d}y'\,{\rm d}z'\\&=\left|\det(\mathbf{T})\right|\int_0^1\int_0^{1-z'}\int_0^{1-z'-y'}\left\{1+\left[{\rm i}(\mathbf{q}\cdot\mathbf{v}_1)x'+{\rm i}(\mathbf{q}\cdot\mathbf{v}_2)y'\right.\right.\\&\quad\left.\left.+{\rm i}(\mathbf{q}\cdot\mathbf{v}_3)z'\right]+{\rm O}(\mathbf{q})\right\}{\rm d}x'\,{\rm d}y'\,{\rm d}z'\\&\simeq\frac{\left|\det(\mathbf{T})\right|}{6}+\left|\det(\mathbf{T})\right|\frac{{\rm i}(\mathbf{q}\cdot\mathbf{v}_1+\mathbf{q}\cdot\mathbf{v}_2+\mathbf{q}\cdot\mathbf{v}_3)}{24}\\&\simeq V_{\rm plhd}+\left|\det(\mathbf{T})\right|\frac{{\rm i}(\mathbf{q}\cdot\mathbf{v}_1+\mathbf{q}\cdot\mathbf{v}_2+\mathbf{q}\cdot\mathbf{v}_3)}{24}. \qquad (17)\end{aligned}$$

To illustrate the loss of arithmetic accuracy near the singularity ($\mathbf{q}=0$), Fig. 4 compares the first-order Taylor expansion (16) with formula (4) for the same tetrahedral form factor as in Fig. 1. For $|\mathbf{q}L|$ close to or below 10^{-4}, results obtained from formula (4) show numeric instabilities owing to the round-off errors near the singularity, while the Taylor expansion (16) works well below 10^{-4}, and there is a range above 10^{-4} where the two methods are in good agreement. Furthermore, only a first-order Taylor expansion is needed for small $\mathbf{q}$.

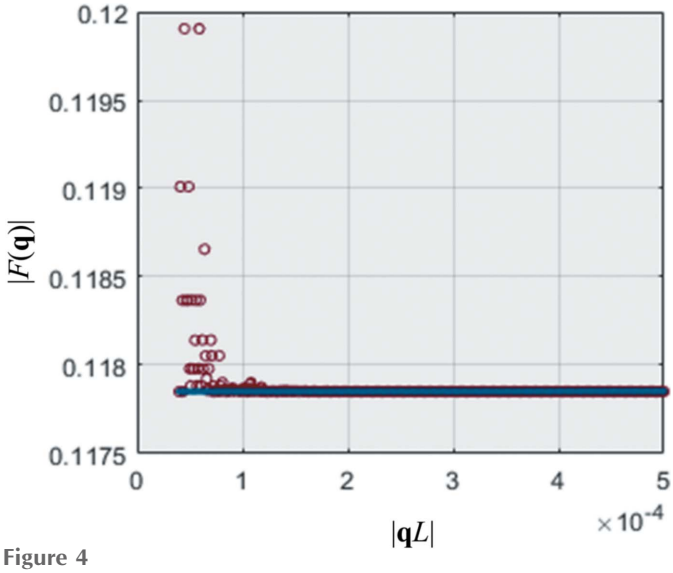

Figure 4
The plot shows the form factor versus $|\mathbf{q}L|$ for the same tetrahedron as in Fig. 1. Red circles are computed using formula (4). For $|\mathbf{q}L|<10^{-4}$, round-off errors dominate. The blue line is computed by the Taylor expansion (16).

Remark 3. Let us summarize Section 3 for reliably computing the form factor at arbitrary wavevectors. The algorithm involves a switch program to check whether formula (4) or a series of variants [equations (10), (12), (14) and (16)] around the singularities were used to compute the form factor. For the basic tetrahedron, we have discussed the $\mathbf{q}$ range to determine which algorithm to use, which is heuristic for computer implementation. Some numerical estimates or a series expansion around singularities being considered to deal with those possible singularities, as described by Wuttke (2021) and Croset (2017), are worthy of mention.

4. The form factor for any polyhedron

Proposition 6. Consider an arbitrary polyhedron given by its K faces Γ_k ($k=1,\ldots,K$) and let each face be an N_k-gon, given by the vertices specified in the sequence $\mathbf{v}_1^k,\mathbf{v}_2^k,\ldots,\mathbf{v}_{N_k}^k$ so that the normal vector of the face Γ_k is outward; then the form factor for the polyhedron is computed from

$$F_{\rm plhd}(\mathbf{q})=\sum_{k=1}^{K}\sum_{i=1}^{N_k-2}\zeta_k^i F_{k\text{-tetra}}^i(\mathbf{q}), \qquad (18)$$

where $F_{k\text{-tetra}}^i(\mathbf{q})$ is the ith tetrahedral form factor based on the kth face of the polyhedron and ζ_k^i is a sign function considering that each tetrahedron can make a positive or negative contribution to the whole integration. Significantly, the normal vector of the face in Proposition 6 points away from the polyhedron; however, the normal vector of the face in Proposition 1 points away from the tetrahedron. They may point in opposite directions. When they point in the same direction, we say that the tetrahedron is positively correlated

with the polyhedron and $\zeta_k^i = 1$; otherwise it has a negative contribution and $\zeta_k^i = -1$.

Proof. According to the linearity property of the Fourier transform, an integral over a polyhedron can be broken into sets of integrals over polygonal cones,

$$F_{\text{plhd}}(\mathbf{q}) = \sum_{k=1}^{K} F_{p\text{-cone}}^{k}(\mathbf{q}), \tag{19}$$

where $F_{p\text{-cone}}^{k}(\mathbf{q})$ is the form factor for the polygonal cone whose base is the face Γ_k of the polyhedron and the tip lies at the origin $\mathbf{v}_0$. Face Γ_k, composed of N_k vertices, can be dissected sequentially into $N_k - 2$ triangles, $T_i^k = \{\mathbf{v}_1^k, \mathbf{v}_{i+1}^k, \mathbf{v}_{i+2}^k\}$, $1 \le i \le N_k - 2$, by taking the vertex $\mathbf{v}_1^k$ as the common vertex of the triangles. Each triangle T_i^k with the origin $\mathbf{v}_0$ forms a tetrahedron $Q_i^k = \{\mathbf{v}_0, \mathbf{v}_1^k, \mathbf{v}_{i+1}^k, \mathbf{v}_{i+2}^k\}$; an integral over a polygonal cone equals the sum of integrals over all tetrahedra:

$$F_{p\text{-cone}}^{k}(\mathbf{q}) = \sum_{i=1}^{N_k-2} F_{k\text{-tetra}}^{i}(\mathbf{q}), \tag{20}$$

where $F_{k\text{-tetra}}^{i}(\mathbf{q})$ is the ith tetrahedral form factor based on the kth face. From formulas (19) and (20), an integral over a polyhedron equals the sum of integrals over all tetrahedra:

$$F_{\text{plhd}}(\mathbf{q}) = \sum_{k=1}^{K} \sum_{i=1}^{N_k-2} F_{k\text{-tetra}}^{i}(\mathbf{q}). \tag{21}$$

Finally, a sign function ζ_k^i is introduced considering that each tetrahedral form factor can make a positive or negative contribution to the whole integral; the integral over the polyhedron equals the sum of the signed integral over each tetrahedron:

$$F(\mathbf{q}) = \sum_{k=1}^{K} \sum_{i=1}^{N_k-2} \zeta_k^i F_{k\text{-tetra}}^{i}(\mathbf{q}). \tag{22}$$

We summarize the proposed method of calculating the form factor of any polyhedron in Fig. 5, which may provide a helpful visualization.

Remark 4. The expression of the polyhedral form factor in its final form involves only the apex coordinates and its topology; there is no need to actually decompose the polyhedron as described above, and the result presented here is consistent with the result given by Croset (2017) who used a different method and vectorial notations in his work.

Remark 5. The use of the scalar product operation and the sign function ζ_k^i in this work allows us to obtain a general and neat formula for any polyhedron, including convex and concave polyhedra.

Remark 6. The total number of computations is linearly proportional to the number of vertices, *i.e.* $2(V - 2)$, where V is the number of vertices of the polyhedron. The computation time can be greatly reduced for a particle with certain symmetries. For instance, assuming that parts P_1 and P_2 are the same size and shape but in different orientations, F_2 can be generated by performing a rotation and translation transformation of F_1, according to the property of the FT

$$F_2(\mathbf{q}) = F_1\left(\mathbf{R}^{-1}\mathbf{q}\right) \exp(i\mathbf{q} \cdot \mathbf{r}), \tag{23}$$

where $\mathbf{r}$ is a shift vector and $\mathbf{R}$ is a rotation matrix used to implement different $\mathbf{q}$ directions.

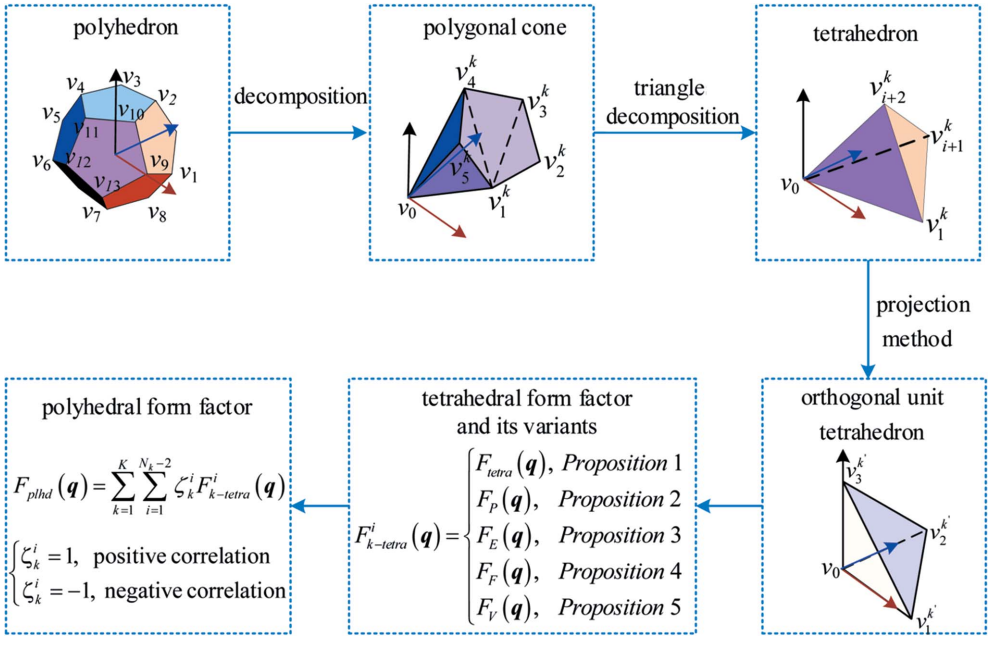

Figure 5
Overview of the proposed method.

5. Illustrative examples

Code for computing the form factor of any polyhedron, based on all the above, has been implemented in a MATLAB program and published at Github (https://github.com/xiuguochen/Small-angle-X-ray-scattering). Several examples were studied in order to verify the accuracy and generality of the method: a cube and a trapezoidal section model have been checked against the reference expressions in an accuracy study. A series of scattering patterns from different particle shapes (regular octahedron, dodecahedron, icosahedron and concave cube) and different **q** directions are discussed as part of a generality study.

5.1. Accuracy test

An accuracy test was performed for a particle shape, the form factor of which can be calculated by direct integration using Fubini's theorem. We now study the well known case of a cube with side lengths $a = 30$ nm, $b = 20$ nm, $h = 40$ nm, having the form factor as formula (24) when oriented as shown in the inset of Fig. 6(a):

$$F(q_x, q_y, q_z) = abh\,\mathrm{sinc}\left(\frac{q_x b}{2}\right) \times \mathrm{sinc}\left(\frac{q_y b}{2}\right)\mathrm{sinc}\left(\frac{q_z b}{2}\right). \tag{24}$$

Since the cardinal sine function $\mathrm{sinc}(x) = \sin(x)/x$ has an analytic continuation at $x = 0$, *i.e.* $\mathrm{sinc}(0) = 1$, the numeric implementation is unproblematic. The code underwent tests for symmetric and asymmetric directions of **q** (along the symmetry axis and off the symmetry axis) to demonstrate the numerical stability. Figs. 6(a) and 6(b) are the two-dimensional reciprocal-space maps (RSMs) in the symmetric and asymmetric directions for the cubic particle, respectively. Figs. 6(c) and 6(d) are comparisons of the scattering intensity between the two methods over a one-dimensional q_x slice, which show good agreement. In order to further illustrate the accuracy of this method, Figs. 6(e) and 6(f) show the absolute errors of the scattering intensity between the two methods in logarithmic form. Both results show that the absolute errors around the singularity ($q_x \to 0$) are much larger than those far from the singularity, but the calculation around the singularity obtained from the proposed method still possesses a high accuracy ($\Delta I < \mathrm{e}^{-10}$).

Fig. 7 presents the case of an isosceles trapezoidal section model with side lengths $a = 30$ nm, $b = 20$ nm, $h = 40$ nm, sidewall angle $\theta = 20°$, having the form factor as formula (25) when oriented as shown in the inset of Fig. 7(a):

$$F(q_x, q_y, q_z) = \left(\frac{\exp(-iq_x a/2)\{\exp[-i(q_y - q_x\tan\theta_2)b] - 1\}}{q_x(q_x\tan\theta_2 - q_y)} + \frac{\exp(iq_x a/2)\{\exp[-i(q_x\tan\theta_1 + q_y)b] - 1\}}{q_x(q_x\tan\theta_1 + q_y)}\right) \times \frac{2\sin(q_z h/2)}{q_z}\exp(iq_y b/2). \tag{25}$$

We also give the two-dimensional RSMs [Figs. 7(a) and 7(b)], comparisons of the scattering intensity over a one-

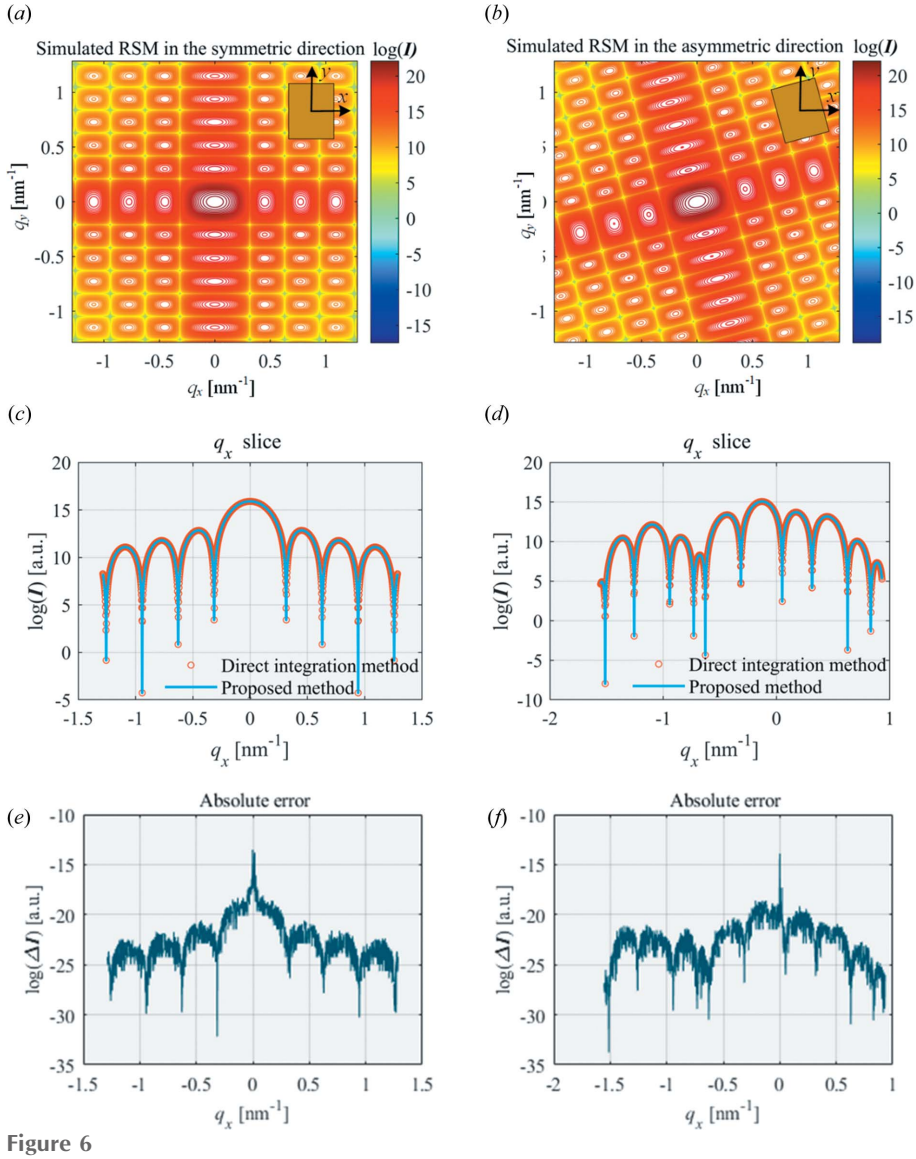

Figure 6
Comparisons of the scattering intensity for a cube between the direct integration method and the proposed method, where the particle is oriented as shown in the inset. (a) and (b) are the two-dimensional RSMs in the symmetric and asymmetric directions; (c) and (d) are comparisons of the scattering intensity between the two methods over the one-dimensional q_x slice; (e) and (f) show the absolute errors of the scattering intensity between the two methods in logarithmic form.

dimensional q_x slice [Figs. 7(*c*) and 7(*d*)] and the absolute errors of the scattering intensity between the two methods [Figs. 7(*e*) and 7(*f*)], for the symmetric and asymmetric directions of **q**. The results show that the calculation around the singularity ($q_x \rightarrow 0$) obtained from the proposed method still possesses a high accuracy ($\Delta I < e^{-10}$), which further demonstrates that the two methods are in good agreement and the proposed method is a reasonable approximation with decent accuracy and numerically stable.

As is evident, the scattering maps from the cube and the isosceles trapezoidal section model display anisotropic scattering behaviours, with higher intensity distributions in the directions perpendicular to the particles' surfaces. This shape-dependent scattering may provide a good criterion to identify particle shape during SAS characterization [for instance, the angle of the line at peak positions in Fig. 7(*a*) corresponds directly to the sidewall angle θ, which provides a simple and intuitive method for extracting the average sidewall angle from the scattering data].

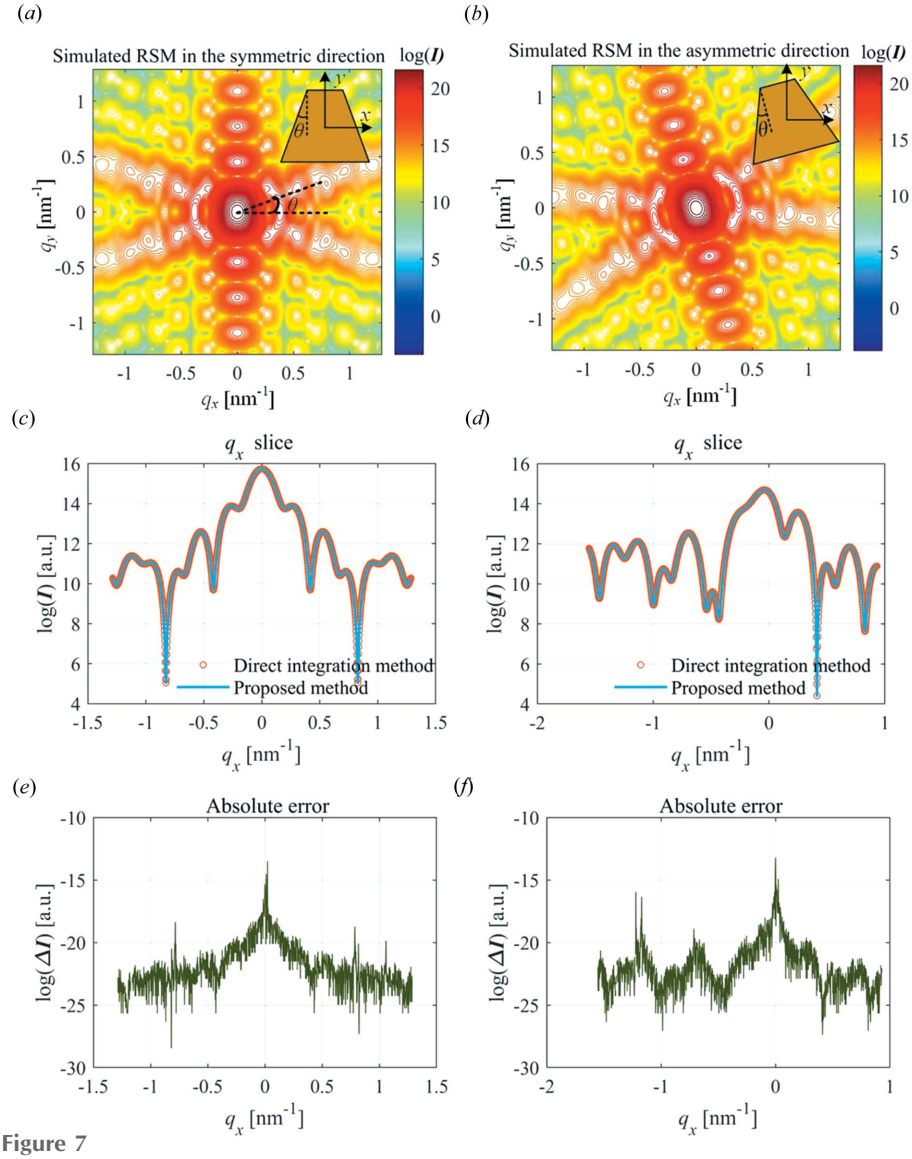

Figure 7
Comparisons of the scattering intensity for an isosceles trapezoidal section model between the direct integration method and the proposed method, where the particle is oriented as shown in the inset. (*a*) and (*b*) are the two-dimensional RSMs in the symmetric and asymmetric directions; (*c*) and (*d*) are comparisons of the scattering intensity between the two methods over the one-dimensional q_x slice; (*e*) and (*f*) show the absolute errors of the scattering intensity between the two methods in logarithmic form.

5.2. Generality test

Upon verifying the accuracy of this method, we think that this approach is valid for any polyhedron including convex and concave polyhedra. We performed generality tests for a suite of particles (octahedron, dodecahedron, icosahedron and a concave cube) and for different **q** directions. The orientations and vertices for these Platonic polyhedra have been defined many times in the literature and will not be repeated here; interested readers are referred to Wolfram (2013). The simulated single-particle scattering pattern (Fig. 8) shows a highly symmetrical scattering feature, with the centre consisting of a series of closed ring features, gradually changing from discontinuous ring features to fringe features, in which structure-related features appear, as described by Barke *et al.* (2015). The scattering of the polyhedron in the low-**q** region shows shape-independent behaviour, while the shape dependence becomes apparent in the high-**q** region. The difference in the scattering behaviour may be used to distinguish particle shape during SAS characterization, provided that the particle can be adequately described by a parametric geometry model.

Again, these patterns present anisotropic scattering distributions. Highly anisotropic particles exhibit more anisotropic behaviours at higher **q**. This can clearly be seen by comparing the maps from the cube and the icosahedron. With the increase of sphericity, the two-dimensional scattering profile appears more isotropic.

It is noteworthy that the scattering of the particle is typically determined by size, shape and orientation. Since we have studied the singularity of $F(\mathbf{q})$ for every direction, we were able to show the dependence of $F(\mathbf{q})$ on the **q** direction. Let us take the dodecahedron as an example. Fig. 9 shows the scattering images under different rotation angles (*i.e.* different **q** directions); the images immediately show different behaviours, demonstrating that the oriented scattering data contain true three-

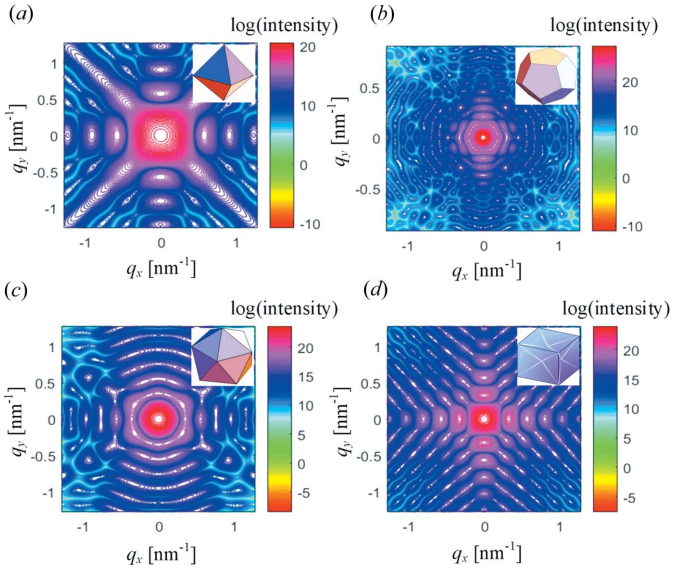

Figure 8
The simulated single-particle scattering images. (*a*) Octahedron, (*b*) dodecahedron, (*c*) icosahedron, (*d*) concave cube.

dimensional structure information. Although the dodecahedron particle becomes more spherical, the scattering images taken for different orientations are extremely diverse. This is what makes diffraction from the dodecahedron different from spherical diffraction – while the scattering from a sphere appears at the same **q** along the different directions, that from a polyhedron depends on both the shape and orientation of the particle. The strong directionality and shape sensitivity (even for nearly spherical shapes) demonstrate that accurate descriptions of particle morphologies will have far-reaching effects on SAS as a characterization tool for studying particle properties.

6. Conclusion

We have shown that the use of a projection method and the sign function allows us to obtain an exact and general form factor of any polyhedron using only the apex coordinates and the apex connections. The obvious singularities are discussed in detail from our formulas [equations (4), (10), (12), (14), (16) and (18)]. The formula is valid for any polyhedron, including the convex polyhedron and the concave polyhedron. Several examples were studied in this work in order to verify the accuracy and generality of the method.

The first advantage of the proposed method is the use of the scalar product operation and the sign function instead of the mixed product (the scalar product and the vector product) as described in previous work, which allows us to obtain a general and neat form factor formula for any polyhedron.

The second advantage of the proposed method is that it has the ability to intuitively identify the direction of the **q** vector in which the singularity appears, and the treatments around the singularities are accurate and numerically stable. Any apparent singularity has been removed and the variants of the form factor have been established analytically.

The third advantage of the proposed method is that the expression of the formula involves only the apex coordinates and their connections, and the implementation of the method is very simple by sequentially scanning over the surfaces of the polyhedron, avoiding the need for decomposition.

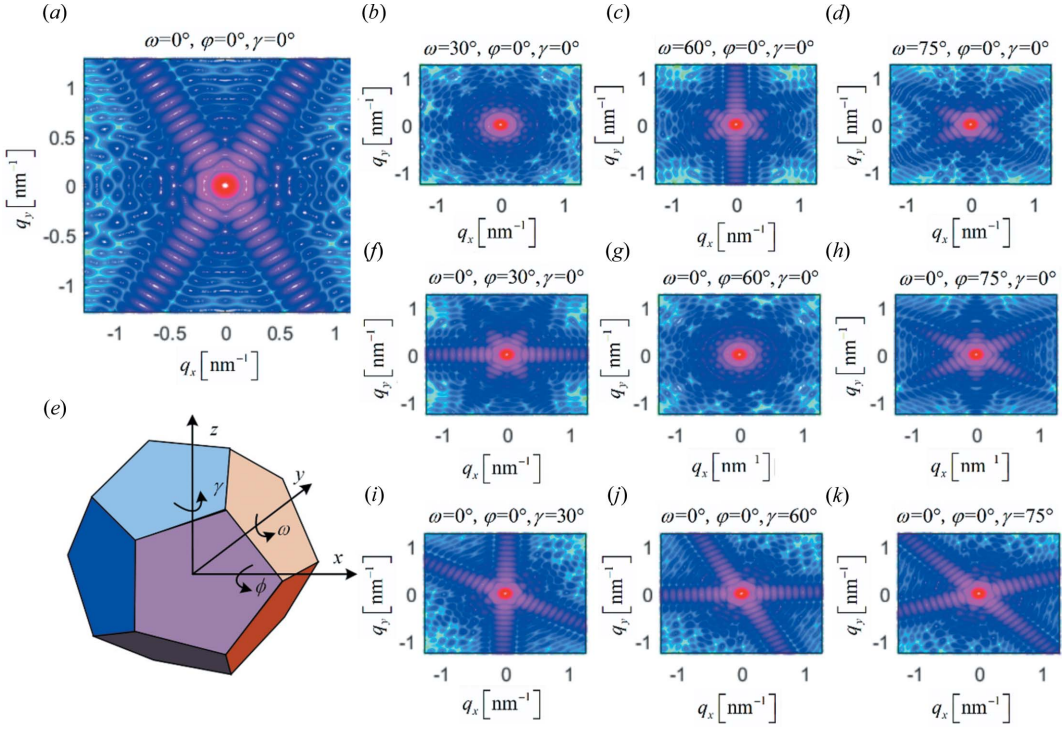

Figure 9
Scattering images of the dodecahedron at different **q** orientations (*i.e.* the particle rotating at different φ, ω, γ angles along the *x*, *y* and *z* axes, respectively).

The ideas presented herein will be useful in the calculation of not only single-particle scattering but also the assembled system made of polyhedral particles. The formulas and discussions presented here are useful for computing the scattering intensities from nanoparticles or clusters, as well as understanding the relevant three-dimensional structure information from scattering patterns. This work will further serve as a stepping-stone for different diffraction modes including transmission, grazing incidence and reflection modes.

Funding information

This work was funded by the National Natural Science Foundation of China (grant Nos. 52022034, 52130504, 62175075) and the Key Research and Development Plan of Hubei Province (2020BAA008).

References

Barke, I., Hartmann, H., Rupp, D., Flückiger, L., Sauppe, M., Adolph, M., Schorb, S., Bostedt, C., Treusch, R., Peltz, C., Bartling, S., Fennel, T., Meiwes-Broer, K. H. & Möller, T. (2015). *Nat. Commun.* **6**, 6187.
Chourou, S. T., Sarje, A., Li, X. S., Chan, E. R. & Hexemer, A. (2013). *J. Appl. Cryst.* **46**, 1781–1795.
Croset, B. (2017). *J. Appl. Cryst.* **50**, 1245–1255.
Croset, B. (2018). *J. Appl. Cryst.* **51**, 1005–1012.
Engel, K. & Laasch, B. (2020). *arXiv*:2011.06971.
Gruner, M. E., Rollmann, G., Entel, P. & Farle, M. (2008). *Phys. Rev. Lett.* **100**, 087203.
Guinier, A. (1963). *J. Chem. Phys.* **79**, 2461–2469.
Guinier, A. & Fournet, G. (1955). *Small-Angle Scattering of X-rays*. New York: John Wiley and Sons Inc.
Hendricks, R. W., Schelten, J. & Schmatz, W. (1974). *Philos. Mag.* **30**, 819–837.
Langille, M. R., Personick, M. L., Zhang, J. & Mirkin, C. A. (2012). *J. Am. Chem. Soc.* **134**, 14542–14554.
Lazzari, R. (2006). *IsGISAXS*. Version 2.6 of 4 May 2006. https://www.insp.upmc.fr/oxydes/IsGISAXS/isgisaxs.htm.
Lee, B., Podsiadlo, P., Rupich, S., Talapin, D. V., Rajh, T. & Shevchenko, E. V. (2009). *J. Am. Chem. Soc.* **131**, 16386–16388.
Lee, Y. T. & Requicha, A. A. G. (1982). *Commun. ACM*, **25**, 642–650.
Li, X., Shew, C.-Y., He, L., Meilleur, F., Myles, D. A. A., Liu, E., Zhang, Y., Smith, G. S., Herwig, K. W., Pynn, R. & Chen, W.-R. (2011). *J. Appl. Cryst.* **44**, 545–557.
Lien, S. L. & Kajiya, J. T. (1984). *IEEE Comput. Graph.* **4**, 35–42.
Mittelbach, P. & Porod, G. (1961). *Acta Phys. Austriaca*, **14**, 185–211.
Murray, C. B., Kagan, C. R. & Bawendi, M. G. (2000). *Annu. Rev. Mater. Sci.* **30**, 545–610.
Patterson, A. L. (1939). *Phys. Rev.* **56**, 972–977.
Pospelov, G., Van Herck, W., Burle, J., Carmona Loaiza, J. M., Durniak, C., Fisher, J. M., Ganeva, M., Yurov, D. & Wuttke, J. (2020). *J. Appl. Cryst.* **53**, 262–276.
Renaud, G., Lazzari, R. & Leroy, F. (2009). *Surf. Sci. Rep.* **64**, 255–380.
Roe, R. J. (2000). *Methods of X-ray and Neutron Scattering in Polymer Science*. New York: Oxford University Press.
Senesi, A. & Lee, B. (2015*a*). *J. Appl. Cryst.* **48**, 565–577.
Senesi, A. J. & Lee, B. (2015*b*). *J. Appl. Cryst.* **48**, 1172–1182.
Warren, B. E. (1990). *X-ray Diffraction*. Mineola: Dover Publications.
Wolfram (2013). *Mathworld*, https://mathworld.wolfram.com/.
Wuttke, J. (2017). *arXiv*:1703.00255.
Wuttke, J. (2021). *J. Appl. Cryst.* **54**, 580–587.
Yamada, Y., Tsung, C. K., Huang, W., Huo, Z., Habas, S. E., Soejima, T., Aliaga, C. E., Somorjai, G. A. & Yang, P. (2011). *Nat. Chem.* **3**, 372–376.